SPECTRAL PROPERTIES AND SOURCE AREAS OF STORM MICROSEISMS AT NORSAR

H. Korhonen, et al

Royal Norwegian Council for Scientific and Industrial Research

Prepared for:

Advanced Research Projects Agency

3 February 1976

NORSAR
ROYAL NORWEGIAN COUNCIL FOR SCIENTIFIC AND INDUSTRIAL RESEARCH

Scientific Report No. 2-75/76

SPECTRAL PROPERTIES AND SOURCE AREAS OF STORM MICROSEISMS AT NORSAR

by

H. Korhonen
Dept. of Geophysics
University of Oulu
Oulu, Finland

and

S. E. Pirhonen
Institute of Seismology
University of Helsinki
Helsinki, Finland

Kjeller, 5 February 1976

Sponsored by
Advanced Research Projects Agency
ARPA Order No. 2551

SECURITY CLASSIFICATION OF THIS PAGE *(When Data Entered)*

REPORT DOCUMENTATION PAGE

READ INSTRUCTIONS BEFORE COMPLETING FORM

1. REPORT NUMBER: F08606-76-C-0001	2. GOVT ACCESSION NO.
3. RECIPIENT'S CATALOG NUMBER	
4. TITLE *(and Subtitle)*: Spectral Properties and Source Areas of Storm Microseisms at NORSAR	5. TYPE OF REPORT & PERIOD COVERED: One-time Technical
6. PERFORMING ORG. REPORT NUMBER: Scientific Report No. 2-75/76	
7. AUTHOR(s): H. Korhonen and S.E. Pirhonen	8. CONTRACT OR GRANT NUMBER(s): F08606-76-C-0001
9. PERFORMING ORGANIZATION NAME AND ADDRESS: NTNF/NORSAR, Postbox 51, 2007 Kjeller, Norway	10. PROGRAM ELEMENT, PROJECT, TASK AREA & WORK UNIT NUMBERS: NORSAR Phase 3
11. CONTROLLING OFFICE NAME AND ADDRESS: VELA Seismological Center, 312 Montgomery Street, Alexandria, Virginia 22314	12. REPORT DATE: 3 February 1976
	13. NUMBER OF PAGES: 38
14. MONITORING AGENCY NAME & ADDRESS *(if different from Controlling Office)*	15. SECURITY CLASS. *(of this report)*
	15a. DECLASSIFICATION/DOWNGRADING SCHEDULE

16. DISTRIBUTION STATEMENT *(of this Report)*

APPROVED FOR PUBLIC RELEASE, DISTRIBUTION UNLIMITED.

17. DISTRIBUTION STATEMENT *(of the abstract entered in Block 20, if different from Report)*

18. SUPPLEMENTARY NOTES

19. KEY WORDS *(Continue on reverse side if necessary and identify by block number)*

Microseisms,

20 ABSTRACT *(Continue on reverse side if necessary and identify by block number)*

Spectral estimates from eight microseismic storms recorded by long period vertical component seismometers at NORSAR exhibit distinct spectral peaks in the bands 50-85 mHz and 110-195 mHz. A high frequency third peak (180-250 mHz) is also resolvable in some cases. High resolution frequency wave-number analysis of the storm microseisms yield azimuthal estimates which are accordant with meteorological disturbances over both the North Atlantic Ocean and the Norwegian Sea. The early stages of a typical storm development

DD FORM 1 JAN 73 1473 EDITION OF 1 NOV 65 IS OBSOLETE

SECURITY CLASSIFICATION OF THIS PAGE *(When Data Entered)*

are characterized by a relatively concentrated microseismic source area to the west of NORSAR, whereas later on the source area expands and new sources appear to the NW and to the north of NORSAR. Simultaneously the spectral peaks migrate towards higher frequencies.

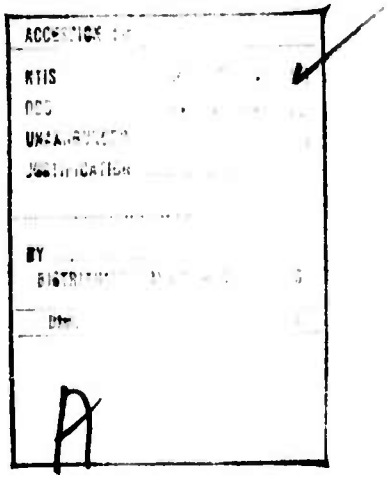

AFTAC Project Authorization No.:		VT/6702/B/ETR
ARPA Order No.	:	2551, Ammendment 8
Program Code No.	:	6F10
Name of Contractor	:	Royal Norwegian Council for Scientific and Industrial Research
Effective Date of Contract	:	1 July 1975
Contract Expiration Date	:	30 June 1976
Contract No.	:	F08606-76-C-0001
Project Manager	:	Nils Marås (02) 71 69 15
Title of Work	:	Norwegian Seismic Array (NORSAR) Phase 3
Amount of Contract	:	$800 000
Contract period covered by the report	:	1 July 1975 - 31 December 1975

This research was supported by the Advanced Research Projects Agency of the Department of Defense and was monitored by AFTAC/VSC, Alexandria VA 22313, under Contract No. F08606-76-C-0001.

CONTENTS

ABSTRACT

Spectral estimates from eight microseismic storms recorded by long period vertical component seismometers at NORSAR exhibit distinct spectral peaks in the bands 50-85 mHz and 110-195 mHz. A high frequency third peak (180-250 mHz) is also resolvable in some cases. High resolution frequency wave-number analysis of the storm microseisms yield azimuthal estimates which are accordant with meteorological disturbances over both the North Atlantic Ocean and the Norwegian Sea. The early stages of a typical storm development are characterized by a relatively concentrated microseismic source area to the west of NORSAR, whereas later on the source area expands and new sources appear to the NW and to the north of NORSAR. Simultaneously the spectral peaks migrate towards higher frequencies.

1. INTRODUCTION

The nature and origins of microseismic waves have been the subject of continuing seismological research for many years. Wiechert (1904) suggested that microseismic waves are generated by the impact of surf against steep coastal areas and thus should exhibit the same periods as the sea waves; however, Bernard (1941) found that microseismic periods are in many cases half of the periods of corresponding sea waves. Significant advances towards a better understanding of the generation mechanisms for these microseismic waves are due to Longuet-Higgins (1950) and Hasselman (1963). Haubrich et al (1963) showed, using seismic and ocean wave recordings from near San Diego, California, that microseismic waves peaked at the same and also at twice the frequency of the corresponding sea waves. They called these types of seismic waves primary frequency (PF) and double frequency (DF) microseisms.

Power spectra of microseisms originated in the North Atlantic Ocean have a similar doubly peaked character (Hinde and Gaunt, 1966; Darbyshire and Okeke, 1969). Analysis of microseisms recorded at Oulu in Finland gave peak frequencies for

PF in the band 70-110 mHz and those of DF microseisms at frequencies over 130 mHz (Korhonen, 1971). These dominant frequencies were found to correlate with those of sea waves recorded at Arviksand near Tromsø in northern Norway. Moreover, at the Oulu seismograph station there have occasionally been observed North Atlantic Ocean microseisms with spectral peaks in the bands 40-60 mHz for PF and 90-130 mHz for DF. In exceptional cases a third peak appeared in the frequency range 180-250 mHz.

Spectral analysis of microseisms has been greatly facilitated with the availability of data recorded (often digitally) at seismic arrays. Furthermore, spatial arrangements of sensors offered the possibility of estimating spatial frequency (wavenumber) spectra in addition to temporal frequencies. Spectral studies of NORSAR microseisms as recorded by long period seismometers are previously published by Capon (1972), Bungum (1974), Korhonen and Pirhonen (1974) and Rygg and Bruland (1974), whereas an earlier study by Bungum et al (1971) included only short period data.

The purpose of this paper is to investigate further the spectral character of storm microseisms at the NORSAR long period array, and the temporal variations of spectra during individual storms and between different storms.

2. DATA AND METHOD OF ANALYSIS

The observational data used in this study are obtained at the NORSAR array and from the weather ships labelled J, I and M in Fig. 1. The long term average of the short period noise level at NORSAR for the year 1972 is shown in Fig. 2 (Bungum 1974), and gives a general view of the noise fluctuations. The numbered arrows and the listed intervals in Fig. 2 indicate the eight microseismic storm periods which are studied in detail in this paper. These storms were selected

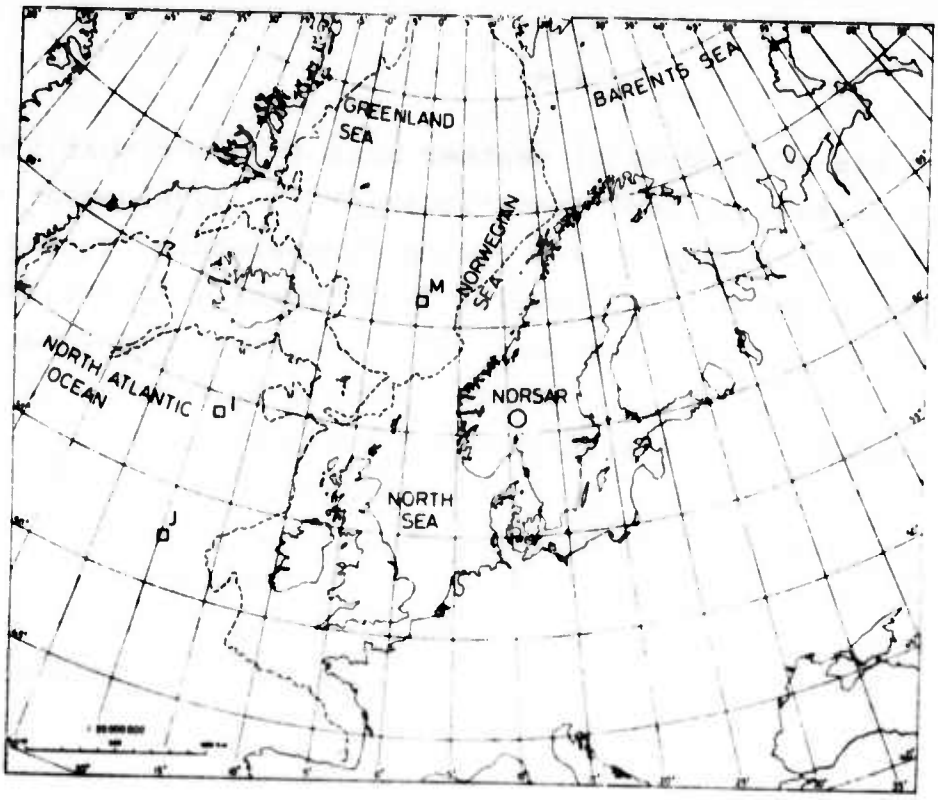

Fig. 1 Locations of NORSAR and weather ships I, J and M. Dotted line indicates the contour for 1000 m sea depth.

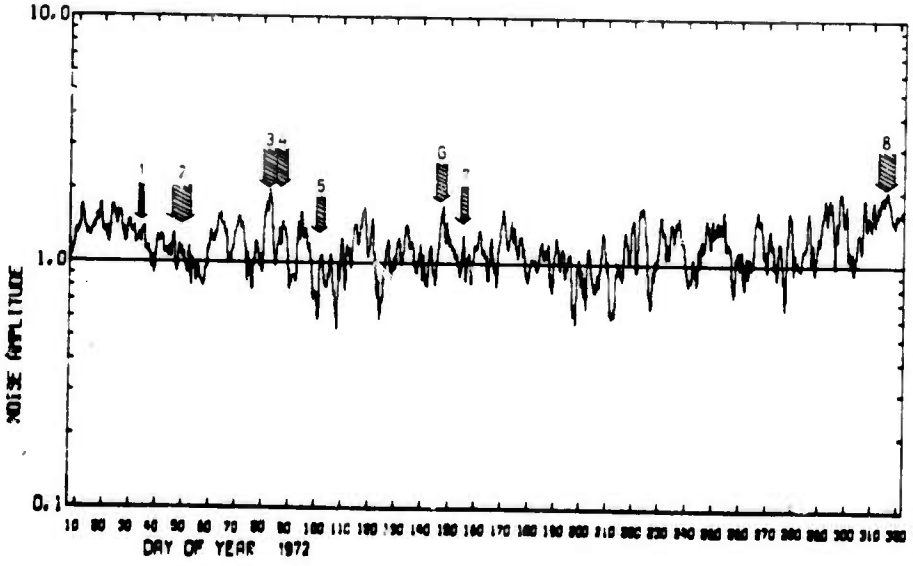

Fig. 2 The long term average of the short period noise level at NORSAR after Bungum (1974). The arrows show the investigated storms, which are as follows:

1.	1972 Feb 2 - 4	Cyclone center over North Atlantic
2.	1972 Feb 15 - 22	Cyclone approaching from Greenland
3.	1972 Mar 20 - 25	Cyclone center over the Norwegian Sea
4.	1972 Mar 26 - 29	Cyclone approaching from North Atlantic
5.	1972 Apr 9 - 12	-"-
6.	1972 May 23 - 27	-"-
7.	1972 Jun 2 - 5	Cyclone center over North Atlantic
8.	1972 Nov 7 - 13	Cyclone center over the Norwegian Sea.

on the basis of studies of weather maps in order that they should represent typical conditions for the development of meteorological storms in and around Fennoscandia. In the northern hemisphere the Coriolis force results in cyclone center movements from the North Atlantic Ocean and towards Fennoscandia. Many of the cyclone centers pass south of Greenland, entering the Norwegian Sea between Iceland and Scotland. This is the case for the storms 4, 5 and 6, while for the storms 1 and 7 the cyclone occludes already over the North Atlantic Ocean before approaching Fennoscandia. For the storms 2, 3 and 8, the cyclone center moves along the northern path from Greenland to northern Fennoscandia and the Barents Sea.

The power spectra in this study were computed from the recordings of NORSAR vertical long period seismographs (see Bungum et al, 1971, for description of NORSAR installation and configuration). A reasonable tradeoff between spectral stability, frequency resolution and computer time requirement has been obtained by averaging spectral estimates from 4 non-overlapping blocks of data, using 256 samples of 1 Hz data per block (Figs. 3a, 3c, 3d, 3g and 3h). This corresponds to 16 degrees of freedom, when block averaging and Hamming smoothing are taken into account, yielding an 80% confidence interval of 4.2 dB and a frequency resolution of 8 mHz. Almost half of the spectra were computed using 10 blocks of data and 128 samples per block, this corresponding to 40 degrees of freedom (Figs. 3b, 3e and 3f). In these cases the 80% confidence interval is 2.5 dB and the frequency resolution is 16 mHz. For each storm, spectral estimates were obtained for total time intervals of 3 or 6 hours. In order to avoid interference from earthquake surface waves, comparisons were always made with photographic records from the nearby high gain ultra long period station at Kongsberg (KON).

Some examples of the computed power spectra are shown in Fig. 3. There is no significant difference between the spectra obtained at different sites within the NORSAR array

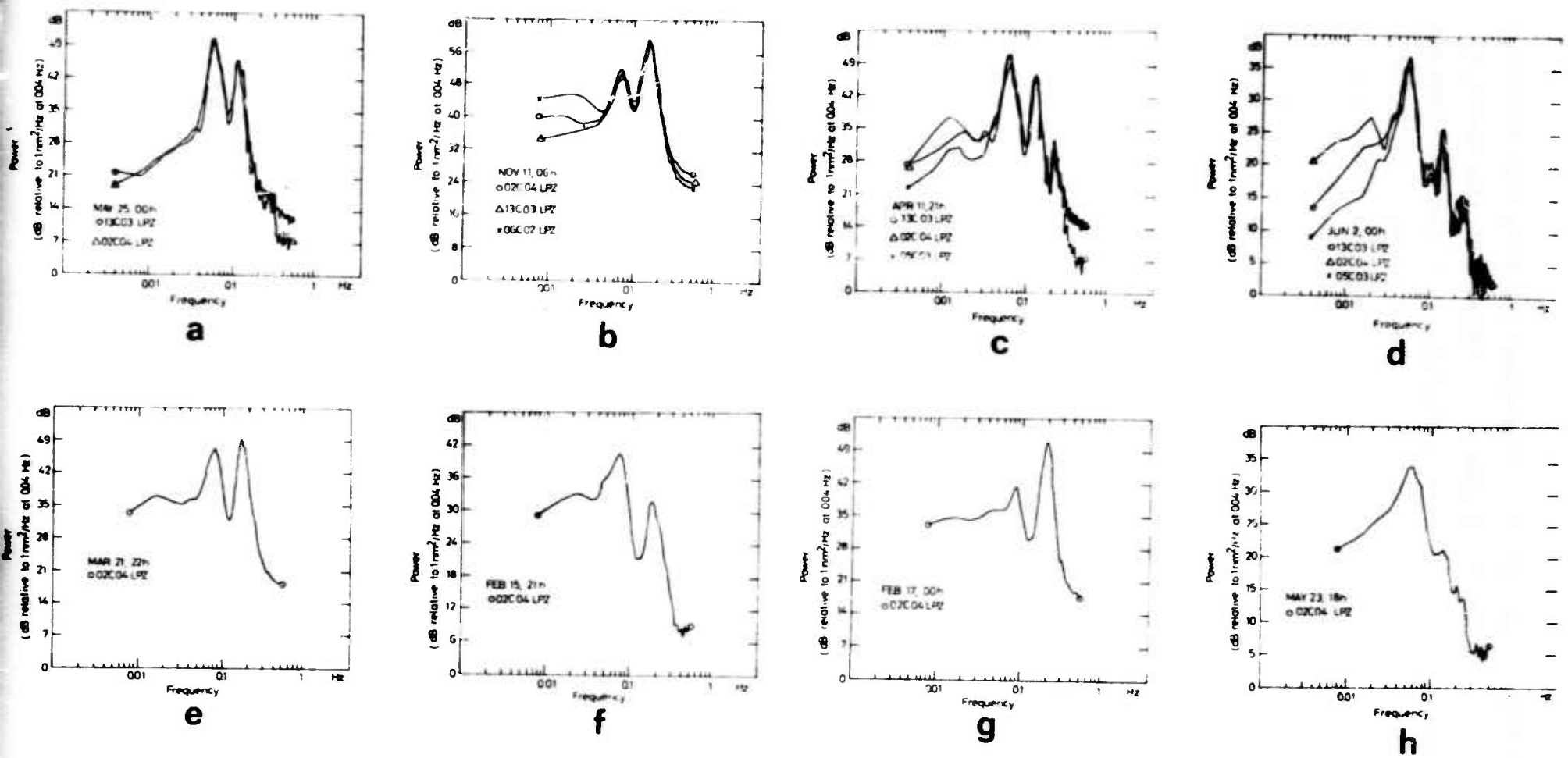

Fig. 3 Typical power spectra computed from NORSAR LP-Z recordings during stormy periods (a-g) and on a quiet day (h). In frames a-d spectra obtained from 2 or 3 different sites within NORSAR are superimposed for comparison. The spectral estimates in frames a, c, d, g, h have 16 degrees of freedom and in frames b, e and f 40 degrees of freedom.

as evident from Figs. 3a-3d. Consequently, only one subarray (02C) was used in the subsequent analysis. All the spectra in Fig. 3 illustrate the peaked character of the microseisms at NORSAR. On a quiet day, however, there appears only one significant peak (above 25 dB; see Fig. 3h). In this case the shape of the spectrum then corresponds to the response curve of the NORSAR LP seismograph system, indicating that the ground spectrum is relatively white. During storm periods, however, at least two peaks are observable and sometimes even a third spectral peak can also be found (see Figs. 3c and 3d).

The main results of the spectral analysis are listed in the Table 1 and 2. The asterisk refers to the spectral estimates with 40 degrees of freedom, while the others have 16. Tables 1 and 2 also contain the spectral character in terms of peak frequencies and peak power values for maxima and minima, where the numbering begins in the low frequency part of the spectrum. The power level and peak frequencies in each case are determined visually from the plotted spectra, read to the closest dB and mHz. As discussed above, the actual resolution is not that good especially in the frequency domain. All the power values in this paper are expressed in dB relative to 1 nm^2/Hz at 0.04 Hz. The spectra are not corrected for instrumental response.

A seismic array such as NORSAR is especially useful for determining directions of approach of microseisms (Bungum, 1974). We have used the high resolution frequency wave-number analysis technique (Capon, 1969), and present the results in terms of wave-number plots as shown in Figs. 4a-4h. In all these cases we used 4 blocks of 256 samples of data from 22 LP-Z sensors giving a frequency resolution of 4 mHz. This analysis essentially provides at selected temporal frequency the power distribution as a function of direction of approach, with the locations of power maxima

Table 1

Power spectral estimates of storms 1, 2, 3 and 4 in order of time. Asterisks designate spectral estimates with 40 degrees of freedom, while others have 16 degrees of freedom.

	DATE	TIME	1. MAXIMUM f mHz	T s	PW dB	1. MINIMUM f mHz	T s	PW dB	2. MAXIMUM f mHz	T s	PW dB
STORM 1.	72-01-31	12h00 *	70	14.3	46	96	10.4	34	138	7.3	44
	72-01-31	18h00 *	55	18.2	46	90	11.1	37	140	7.1	43
	72-02-01	18h00 *	55	18.2	49	92	10.9	38	130	7.7	45
	72-02-02	00h00	56	17.9	50	94	10.6	35	120	8.3	45
	72-02-02	06h00	57	17.5	52	94	10.6	35	115	8.7	43
	72-02-02	12h00	59	17.0	50	92	10.9	31	118	8.5	46
	72-02-02	18h00	59	17.0	52	92	10.9	35	122	8.2	44
	72-02-03	00h00	57	17.5	51	93	10.8	34	121	8.3	43
	72-02-03	05h00	63	15.9	46	94	10.6	32	133	7.5	45
	72-02-03	12h00	64	15.6	47	102	9.8	30	145	6.9	47
	72-02-03	18h00	64	15.6	45	100	10.0	31	133	7.5	51
	72-02-03	23h00	63	15.9	43	98	10.2	29	136	7.4	49
	72-02-04	00h00	63	15.9	46	94	10.6	30	137	7.3	47
	72-02-04	04h00	65	15.4	46	100	10.0	32	135	7.4	48
	72-02-04	08h00	63	15.9	43	98	10.2	29	125	8.0	45
	72-02-04	19h00	63	15.9	46	102	9.8	30	130	7.7	41
STORM 2.	72-02-15	21h00 *	74	13.5	41	125	8.0	21	176	5.7	32
	72-02-16	02h00 *	70	14.3	43	125	8.0	23	180	5.6	33
	72-02-16	06h00 *	74	13.5	42	127	7.9	24	167	6.0	37
	72-02-16	12h00 *	80	12.5	44	124	8.1	28	203	4.9	44
	72-02-16	20h00 *	79	12.7	44	120	8.3	31	195	5.1	49
	72-02-17	00h00	84	11.9	42	120	8.3	30	195	5.1	51
	72-02-17	06h00	80	12.5	38	120	8.3	24	196	5.1	45
	72-02-17	12h00	76	13.2	39	129	7.8	22	215	4.7	41
	72-02-17	18h00	70	14.3	38	117	8.6	24	180	5.6	35
	72-02-18	00h00	70	14.3	45	112	8.9	26	154	6.5	41
	72-02-18	06h00	72	13.9	42	113	8.9	25	146	6.9	45
	72-02-18	12h00	66	15.2	45	115	8.7	26	152	6.6	42
	72-02-18	15h00	72	13.9	46	118	8.5	26	166	6.0	42
	72-02-18	19h00	66	15.2	46	116	8.6	26	156	6.4	44
	72-02-19	00h00	68	14.7	49	105	9.5	32	142	7.0	48
	72-02-19	06h00	64	15.6	51	106	9.4	28	138	7.3	46
	72-02-19	12h00	60	16.7	53	100	10.0	34	133	7.5	46
	72-02-19	19h00	67	14.9	46	107	9.4	29	137	7.3	43
	72-02-19	22h00 *	66	15.1	38	106	9.4	29	139	7.2	34
	72-02-20	04h00 *	66	15.2	44	109	9.2	28	148	6.8	41
	72-02-20	12h00 *	66	15.2	44	109	9.2	29	150	6.7	42
	72-02-20	18h00 *	67	14.9	43	110	9.1	29	156	6.4	41
	72-02-21	00h00 *	63	15.9	46	105	9.5	33	156	6.4	38
	72-02-21	04h00 *	63	15.9	46	102	9.8	33	128	7.8	39
STORM 3.	72-03-21	08h00 *	86	11.6	36	133	7.5	23	190	5.3	37
	72-03-21	15h00	82	12.2	46	113	8.9	29	172	5.8	49
	72-03-21	22h00 *	78	12.8	47	117	8.6	32	164	6.1	49
	72-03-22	07h00 *	78	12.8	46	109	9.2	34	156	6.4	48
	72-03-22	20h00 *	70	14.3	47	109	9.2	36	164	6.1	50
	72-03-23	06h30 *	63	15.9	58	100	10.0	45	141	7.1	62
	72-03-23	16h00	66	15.2	58	98	10.2	38	141	7.1	65
	72-03-24	00h00 *	72	13.9	52	109	9.2	38	156	6.4	56
	72-03-24	12h00	74	13.5	45	121	8.3	26	160	6.3	50
	72-03-24	15h02	74	13.5	41	125	8.0	25	160	6.3	46
	72-03-24	22h00 *	75	13.3	38	120	8.3	28	172	5.8	41
	72-03-25	09h00 *	86	11.6	35	117	8.6	26	180	5.6	38
	72-03-25	10h00 *	86	11.6	36	125	8.0	26	180	5.6	36
	72-03-25	20h00 *	78	12.8	34	113	8.9	25	180	5.6	33
STORM 4.	72-03-26	07h00 *	55	18.2	41	109	9.2	28	154	6.5	34
	72-03-26	12h00 *	63	15.9	46	98	10.2	36	120	8.3	45
	72-03-26	18h00 *	60	16.7	50	92	10.9	39	117	8.6	50
	72-03-27	00h00 *	58	17.2	51	88	11.4	39	118	8.5	52
	72-03-27	06h00 *	62	16.1	54	92	10.9	40	125	8.0	53
	72-03-27	09h50 *	61	16.4	54	95	10.5	40	128	7.8	52
	72-03-27	15h00 *	62	16.1	54	92	10.9	38	126	7.9	51
	72-03-27	21h00 *	65	15.4	53	99	10.1	41	130	7.7	51
	72-03-28	00h00	64	15.6	55	100	10.0	36	128	7.8	53
	72-03-28	06h00	66	15.2	51	100	10.0	34	130	7.7	49
	72-03-28	10h40	70	14.3	49	100	10.0	30	134	7.5	46
	72-03-28	12h00	67	14.9	48	105	9.5	30	135	7.4	44
	72-03-28	22h00	66	15.2	45	115	8.7	25	156	6.4	38
	72-03-29	03h00	70	14.3	42	112	8.9	25	178	5.6	40
	72-03-29	09h00	74	13.5	41	117	8.6	24	170	5.9	39
	72-03-29	15h00	78	12.8	36	125	8.0	21	180	5.6	37
	72-03-29	20h00	80	12.5	35	140	7.1	19	180	5.6	33

Table 2

Power spectral estimates of storms 5, 6, 7 and 8 in order of time. Asterisks designate spectral estimates with 40 degrees of freedom, while others have 16 degrees of freedom.

			1. MAXIMUM			1. MINIMUM			2. MAXIMUM			2. MINIMUM			3. MAXIMUM		
	DATE	TIME	f mHz	T s	PW dB	f mHz	T s	PW dB	f mHz	T s	PW dB	f mHz	T s	PW dB	f mHz	T s	PW dB
STORM 5.	72-04-09	00h00	55	18.2	34	109	9.2	21	129	7.8	25						
	72-04-09	15h00	55	18.2	33	109	9.2	22	145	6.9	33						
	72-04-09	18h00	51	19.6	37	109	9.2	22	156	6.4	36						
	72-04-09	21h00	70	14.3	35	105	9.5	28	148	6.8	36						
	72-04-10	00h00	63	15.9	35	105	9.5	24	141	7.1	36						
	72-04-10	12h00	59	17.0	52	90	11.1	38	121	8.3	54						
	72-04-11	00h00	55	18.2	55	94	10.6	30	117	8.6	51	184	5.4	29	215	4.7	37
	72-04-11	10h00	59	17.0	56	90	11.1	34	117	8.6	50	176	5.7	29	211	4.7	41
	72-04-11	15h00	55	18.2	54	90	11.1	32	117	8.6	48	176	5.7	26	207	4.8	36
	72-04-11	17h00	55	18.2	53	98	10.2	34	125	8.0	47	176	5.7	26	207	4.8	36
	72-04-11	21h00	63	15.9	50	94	10.6	29	129	7.8	47	188	5.3	23	211	4.7	33
	72-04-12	00h00	63	15.9	46	102	9.8	28	129	7.8	44	191	5.2	23	215	4.7	29
	72-04-12	09h30	70	14.3	44	109	9.2	21	152	6.6	37						
	72-04-12	15h00	70	14.3	38	109	9.2	19	160	6.3	31						
	72-04-12	21h00	78	12.8	37	113	8.9	17	152	6.6	27						
STORM 6.	72-05-25	00h00	55	18.2	51	86	11.6	32	109	9.2	45						
	72-05-25	06h00	58	17.2	55	83	12.1	42	110	9.1	57						
	72-05-25	12h00	59	17.0	57	86	11.6	36	115	8.7	58						
	72-05-25	18h00	59	17.0	56	88	11.4	34	119	8.4	56						
	72-05-26	00h00	55	18.2	58	90	11.1	38	120	8.3	50						
	72-05-26	06h00	59	17.0	54	90	11.1	40	109	9.2	55						
	72-05-26	12h00	59	17.0	58	90	11.1	38	113	8.9	58						
	72-05-26	18h00	57	17.5	54	94	10.6	39	118	8.5	53						
	72-05-27	00h00	60	16.7	50	102	9.8	34	126	7.9	50						
	72-05-27	06h00	65	15.4	49	102	9.8	30	137	7.3	43	180	5.6	24	219	4.6	32
	72-05-27	21h00	66	15.2	40	98	10.2	27	141	7.1	38	180	5.6	31	205	4.9	37
STORM 7.	72-06-02	00h00	54	18.5	36	0	0.0	00	137	7.3	26						
	72-06-02	06h00	55	18.2	36	90	11.1	17	137	7.3	25						
	72-06-02	12h00	52	19.2	38	90	11.1	16	133	7.5	26						
	72-06-02	19h00	53	18.9	38	113	8.9	18	141	7.1	28						
	72-06-03	02h00	55	18.2	37	109	9.2	18	141	7.1	28						
	72-06-03	05h30	74	13.5	41	109	9.2	17	156	6.4	31						
	72-06-03	10h00	74	13.5	43	113	8.9	24	148	6.8	34						
	72-06-03	14h00	72	13.9	45	109	9.2	25	145	6.9	35						
	72-06-03	18h00	74	13.5	44	107	9.4	25	152	6.6	42						
	72-06-04	00h00	70	14.3	45	117	8.6	24	156	6.4	41						
	72-06-04	06h00	67	14.9	43	113	8.9	26	160	6.3	4[illegible]						
	72-06-04	14h00	70	14.3	44	113	8.9	26	152	6.6	41						
	72-06-04	16h00	78	12.8	42	113	8.9	21	160	6.3	40						
	72-06-04	22h40 *	74	13.5	38	117	8.6	23	160	6.3	34						
	72-06-05	03h00 *	76	13.2	36	117	8.6	21	166	6.0	31						
	72-06-05	06h00 *	78	12.8	33	120	8.3	21	166	6.0	29						
STORM 8.	72-11-06	03h00 *	61	16.4	43	102	9.8	37	128	7.8	44						
	72-11-06	10h00 *	57	17.5	47	100	10.0	35	130	7.7	43						
	72-11-06	14h00 *	55	18.2	48	103	9.7	36	131	7.6	40						
	72-11-06	18h00 *	52	19.2	50	123	8.1	38	138	7.3	40						
	72-11-06	22h00 *	53	18.9	54	80	12.5	44	107	9.4	52						
	72-11-07	12h00 *	54	18.5	63	82	12.2	54	107	9.4	65						
	72-11-08	00h00 *	57	17.5	62	81	12.4	52	112	8.9	67						
	72-11-08	06h00 *	58	17.2	61	88	11.4	49	116	8.6	64						
	72-11-08	11h50 *	61	16.4	59	89	11.2	47	122	8.2	60						
	72-11-08	18h00 *	65	15.4	56	99	10.1	45	132	7.6	58						
	72-11-09	00h00 *	66	15.2	54	103	9.7	41	148	6.8	55						
	72-11-09	13h00 *	71	14.1	52	107	9.4	36	150	6.7	53						
	72-11-10	00h00 *	75	13.3	50	111	9.0	36	165	6.1	50						
	72-11-10	06h00 *	68	14.7	48	111	9.0	38	172	5.8	53						
	72-11-10	11h00 *	69	14.5	51	108	9.3	39	170	5.9	52						
	72-11-10	18h00 *	68	14.7	55	101	9.9	41	156	6.4	58						
	72-11-11	00h00 *	68	14.7	53	102	9.8	39	158	6.3	58						
	72-11-11	06h00 *	72	13.9	50	100	10.0	44	150	6.7	59						
	72-11-11	11h00 *	70	14.3	50	102	9.8	42	150	6.7	59						
	72-11-12	00h00 *	68	14.7	45	105	9.5	37	163	6.1	50						
	72-11-12	06h00 *	66	15.2	46	107	9.4	34	160	6.3	47						
	72-11-12	12h00 *	65	15.4	47	107	9.4	33	159	6.3	45						
	72-11-13	00h00 *	65	15.4	46	105	9.5	35	150	6.7	47						
	72-11-13	18h00 *	67	14.9	45	106	9.4	32	152	6.6	46						

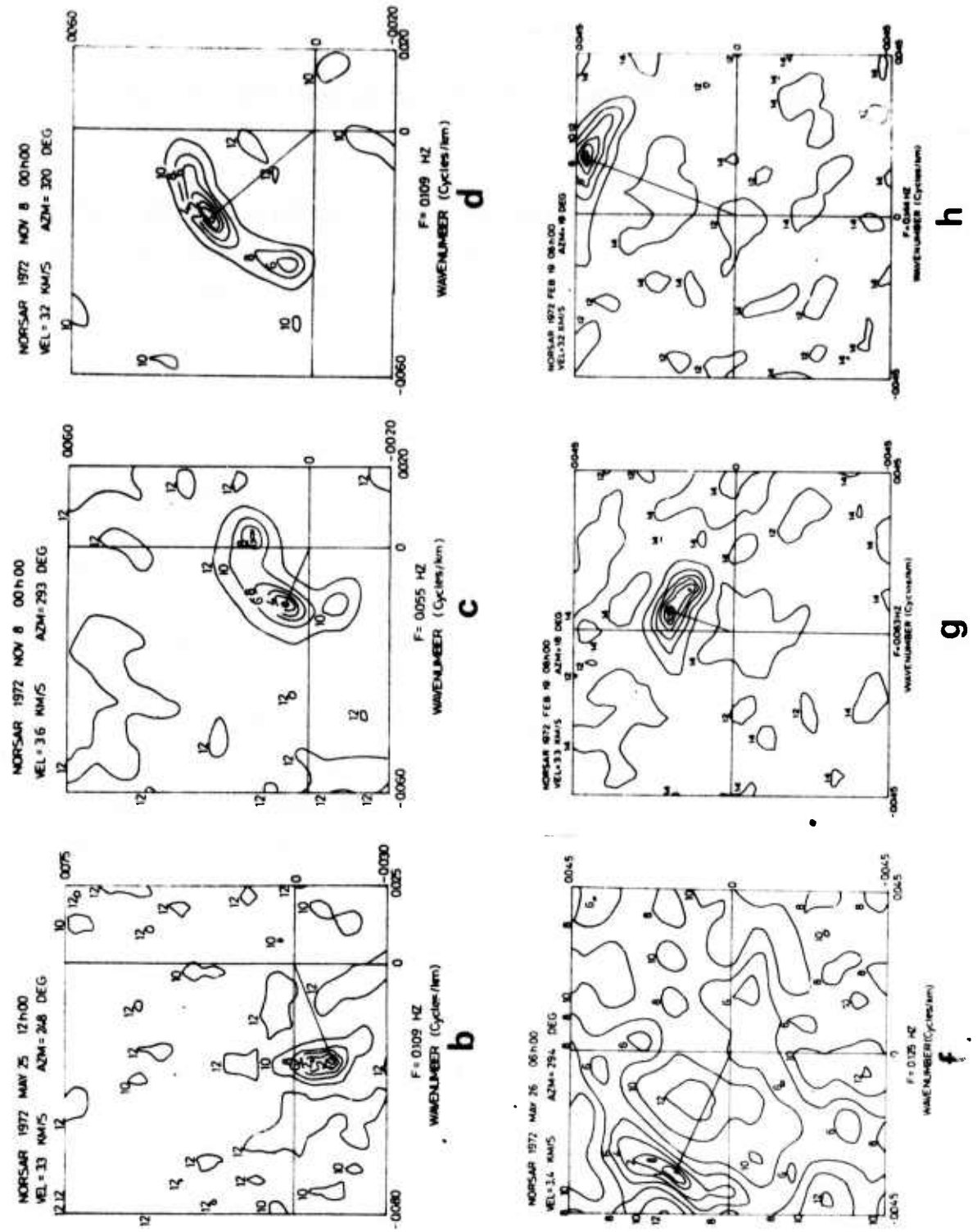

Fig. 4 Wave-number spectra for the 1st and 2nd peak frequencies for four different storms.

giving estimates of phase velocity and direction of most coherent arrivals.

The frequency wave-number spectra were computed for different time intervals during the development of each storm, and for the peak frequencies inferred from the power spectra. The direction of approach and phase velocities for each peak frequency determined in this way are tabulated in Table 3. The uncertainties are here more difficult to assess, but following Bungum and Capon (1974) one can say that they are not less than $\pm 5^{\circ}$ in azimuth and ± 0.3 km/s in phase velocity. An asterisk in this table indicates cases when the noise is relatively equally distributed over a wide azimuthal range the given azimuth being the direction towards the power maximum. A similar azimuthal spread can of course be inferred for the noise sources. On May 26, 0600 GMT, the wave-number spectrum was also computed at the frequency of the minimum between the 1st and 2nd peak. Experimentally, it was found that the wave field of the high frequency third peak could not be resolved because of the instrument response at these frequencies. Thus for these frequencies the high resolution analysis was applied instead to the recordings of one short period subarray, with corresponding significant drop in estimation accuracy (only six SP sensors within a subarray). Also these results are indicated in Table 3.

Table 3

Microseism source locations of the eight storms analyzed in terms of azimuth and phase velocity of the power maximum in wave-number space for selected peak frequencies and for selected time intervals. Asterisks indicate significant microseismic energy approaching from different directions.

	DATE	TIME	PEAK 1. f mHz	AZM n°	VEL km/s	PEAK 2. f mHz	AZM n°	VEL km/s	PEAK 3. f mHz	AZM n°	VEL km/s
STORM 1.	72-02-02	12h00	55	233*	3.6	117	260	3.2			
	72-02-03	18h00	63	260*	3.4	132	274	3.4			
STORM 2.	72-02-16	12h00	75	13	3.3	179	260	3.2			
	72-02-17	00h00	85	11	3.3	184	285	3.2			
	72-02-18	06h00	73	15	3.3	147	15	3.3			
	72-02-19	06h00	63	16	3.3	144	19	3.2			
	72-02-20	12h00	60	310	3.5	150	332	3.2			
	72-02-21	04h00	60	256	3.6	119	268	3.2			
STORM 3.	72-03-21	22h00	70	294*	3.6	159	284	3.2			
	72-03-22	20h00				169	351	3.2			
	72-03-23	16h00	70	284*	3.4	139	324	3.3			
	72-03-23	09h00							219	309	3.5
	72-03-24	00h00	70	294*	3.6						
	72-03-24	22h00	75	338	3.5	169	342	3.2			
STORM 4.	72-03-27	00h00	65	254	3.5	130	263	3.3			
	72-03-28	00h00	60	288	3.8	119	310*	3.1			
	72-03-29	03h00	70	288*	3.6	168	300	3.2			
STORM 5.	72-04-10	13h45	59	255	3.5	121	263	3.3	230	263	3.1
	72-04-11	00h00	55	281	3.5	117	265	3.2	233	263	3.2
STORM 6.	72-05-25	12h00	55	263	3.2	109	248	3.3			
	72-05-26	06h00	63	360*	3.5	125	294	3.4			
	72-05-26	06h00	1. minimum			82	261	3.8			
	72-05-27	00h00	60	2*	3.2	130	317*	3.2	200	242	3.2
STORM 7.	72-06-02	12h00	63	306	4.1						
	72-06-02	18h45							239	257	3.2
	72-06-03	10h00	70	255*	3.4	150	250	3.2			
	72-06-04	00h00	73	254*	3.3	155	288	3.2			
	72-06-04	16h00	70	284*	3.4	150	281	3.3	244	358	3.3
STORM 8.	72-11-06	14h00	55	300	3.4	114	254	3.4	175	350	3.2
	72-11-06	22h00	55	285	3.5	114	252	3.3	175	21	2.6
	72-11-08	00h00	55	293*	3.6	109	320	3.2			
	72-11-09	13h00	70	360*	3.3	147	293	3.2			
	72-11-10	11h00	70	259	3.4	159	279	3.3			
	72-11-11	11h00	70	296*	3.4	147	356	3.2			
	72-11-11	12h00	75	360*	3.8	125	360	3.1			
	72-11-12	12h00	70	343*	3.4	164	23	3.2			

3. RESULTS AND DISCUSSION

3.1 General Description

A general overview of the spectral development of the microseismic storms can be obtained by presenting the results from successive power spectra analyses in terms of sonograms as shown in Figs. 5a-12a, where power contours are drawn at intervals of 5 dB. The essential information from the power spectra is also given in Figs. 5b-12b, where the periods of 1st and 2nd peak are displayed. Also given on each of these figures is a curve at half the period (double frequency) of the 1st peak, to be compared with the observed values for the 2nd peak. Remembering the frequency resolution of our estimates, which in the best case corresponds to an uncertainty of ± 0.5 sec for the 6-8 sec waves, differences in the peak periods of less than about 1.0 sec are not significant. On the same figures (5b-12b) the main direction of approach of microseismic waves is shown by full line arrows. The dotted line arrows indicate directions of approach from simulataneous additional sources.

For all the storms investigated representative weather maps (from the Finnish Meteorological Institute) are included in Figs. 5c-12c. More detailed information about wind and sea wave data are given in Figs. 5d-12d, with observations from the North Atlantic weather ships J, I or M (Schiffsbeobachtungen, Täglicher Wetterbericht des Deutschen Wetterdienstes, Frankfurt, a.M.). In order to make easier a comparison between the weather ship data and the microseismic data, those figures also contain the seismic peak power values in dB for the 1st and 2nd peaks. The wind velocity maxima during these storms are from 40 to 60 knots, wind direction being mostly between W and SW. Consequently, the wind, the sea waves and the swell are running towards the coastal areas of the British Isles and towards the Norwegian west coast. In some cases waves towards Iceland are evident. Wave period measurements made visually at the weather ships are

not accurate enough for detailed comparison between microseismic and sea wave periods. For such purposes, the ground motion microseismic spectra and continuous sea wave recordings, which have not been available for this study, are essential. A more detailed discussion of the generation mechanisms for microseisms would be dependent on the availability of such data.

3.2 Individual Storms

Storm 1. 1972 February 1-4, Fig. 5

The storm starts with a noticeable increase of power at low frequencies around 55-60 mHz. The power of the 2nd peak is initially about 5 dB below the 1st peak (Fig. 5a and 5d). We remark, however, that the instrument response at 8 sec is 15 dB below that at 16 sec, so in the ground motion spectra the 2nd peak is the strongest one. The wave-number analysis shows on February 2 coherent waves approaching mainly from SW but a low frequency microseismic source is also evident to the north of NORSAR. This is suggestive of North Atlantic swell approaching the Norwegian coast. On February 3 the main direction of microseisms is westward for both of the peaks. The expected and observed 2nd peak frequencies coincide very well after February 2. The source area of this microseismic storm seems to be mainly in the North Atlantic Ocean to the west of the British Isles, but the cold front belonging to the depression and also the swell may generate microseisms at the Norwegian coast in the later part of the storm development.

Storm 2. 1972 February 16-21, Fig. 6

During this storm the power level of 1st and 2nd peaks remains nearly equal except on February 18, when the first peak is about 5 dB above the 2nd peak. The direction of approach is mostly from N and NNE, but in the beginning of this storm the 2nd peak microseisms seem to be approaching

from W. These microseisms might be generated at the coastal areas of Iceland, whereas the other part of the microseisms for this storm seem to be generated at the northern coasts of Norway near the deep water boundary between Lofoten and Svalbard. This storm is the only case in which the microseisms are approaching from NE, which may suggest that the areas in and around the Barents Sea are not favorable for the generation of microseisms. In the end of this storm period the frequency wave-number spectra show a direction of approach from W, which may be due to a new storm approaching from the North Atlantic Ocean.

Storm 3. 1972 March 21-25, Fig. 7

This storm is typical for the cases in which the sources are in the Norwegian Sea and the coastal waters. It is interesting to note the U-shaped character of the sonogram; with increasing power the peak frequencies change towards lower frequencies and vice-versa. The maximum power in this case is very high, about 60 dB, the 2nd peak being all the time at a higher level than the 1st. The direction of approach is between N and NW.

Storm 4. 1972 March 25-29, Fig. 8

This storm shows how the microseisms change when the source, in this case a strong cyclone center, moves from the North Atlantic Ocean into the Norwegian Sea and further across Fennoscandia. The direction of approach is mostly from west for both peaks. On March 29, however, a secondary source appears to the north of NORSAR in the same way as for storm 1. The periods are decreasing with time as the storm develops. The rapid decrease of the power level when the storm center moves inland is also noteworthy.

Storm 5. 1972 April 8-12, Fig. 9

This storm is approaching Fennoscandia from south of Iceland, and has a rather sudden beginning in the afternoon of April 9. The spectra exhibit a migration of peak frequencies towards lower values. The wave-number analysis indicates well-concentrated maxima to the west of NORSAR suggesting that the associated source area may be located west of the British Isles. Later a 3rd peak occurs in the 200-250 mHz band, for which the corresponding microseisms are approaching from the same direction as those of the other peaks.

Storm 6. 1972 May 23-27, Fig. 10

This storm begins with a rapid increase in the power of the 2nd peak on May 25. In the end of this day the power of the 2nd peak decreases and the 1st peak dominates. Simultaneously the wave-number spectrum shows a change of direction from W to N for the main part of 1st peak microseisms. Later also the 2nd peak microseisms changes their direction of approach from W to NW. A wave-number spectrum computed at the frequency of the minimum between 1st and 2nd peaks shows the direction of approach from the west, as in the case of the 2nd peak microseisms.

At the beginning of May 26 the frequency of the 2nd peak changes rapidly. This could be due to the source area changing from the North Atlantic Ocean into the Norwegian Sea. Towards the end of this storm there occurs also a third peak in the high frequency part of the spectrum, with frequencies in the band 200-220 mHz and with power levels of 30-36 dB.

Storm 7. 1972 June, Fig. 11

This is a special case representing a summer storm. The power remains at significantly lower levels than during non-summer storms. It begins with a power maximum at the 1st peak. The peak frequencies are also higher than during most of the other storms, with 75 mHz for the 1st peak and 150 mHz for the 2nd peak at the time of the storm maximum. The

sudden change in peak frequencies on June 3 may reflect a corresponding change in source areas from the North Atlantic Ocean into the Norwegian Sea.

Storm 8. 1972 November 6-13, Fig. 12

This is an example of strong storms which occur often in late autumn. The storm is characterized by two microseismic maxima, the first occurring Nov 7-Nov 8, the second Nov 10-Nov 11. These may be due to different cyclones approaching nearly along the same path from Greenland to Fennoscandia. In both cases the direction of approach of the microseisms is at first from W, and later the main source appears to the NW and then to the N of NORSAR. The wind velocity and wave height plots in Fig. 12d also indicate two successive maxima at weather ship J, but these do not correlate with the microseismic power at NORSAR as well as in the other cases. The 2nd peak is the strongest one, with an unusually high maximum of 67 dB at a frequency of 112 mHz on Nov 7. At the same time the 1st peak reaches a maximum of 63 dB at a frequency of 54 mHz. Later both of these peaks shift towards lower frequencies and their power decreases 10-15 dB. Sea wave spectra for Nov 7 published by Rygg and Bruland (1974) show waves at the Norwegian coast peaking at periods of nearly 18 sec and 8 sec. The latter periods are presumably connected to the distant swell, which according to Fig. 12d is running towards the Norwegian coast. The microseismic waves from this storm may be generated mainly in the Norwegian Sea and at the Norwegian coast.

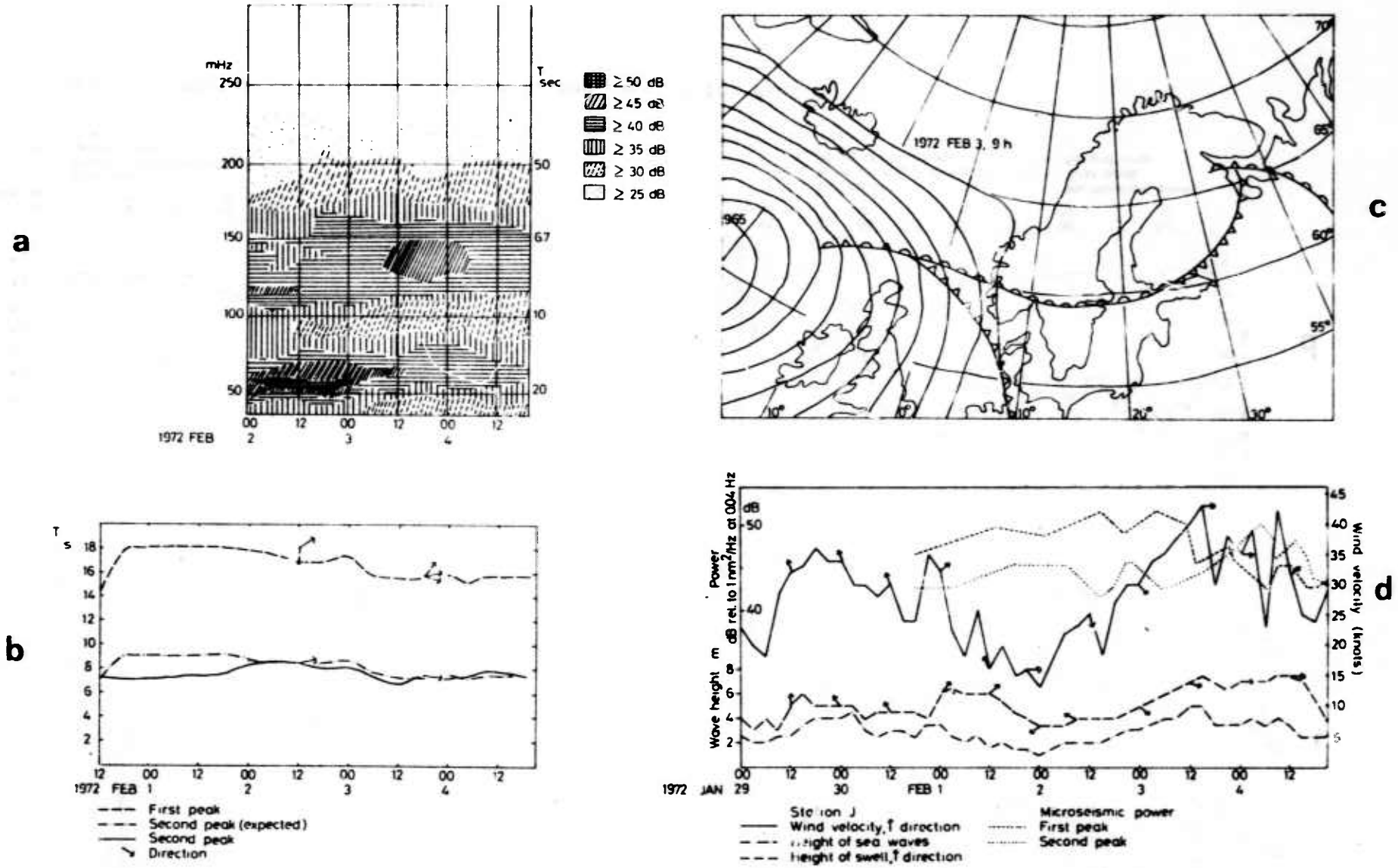

Fig. 5 Pictorial synopsis of storm 1. a) Sonogram illustrating power spectral variations during storm progression. b) Variation with storm progression of the periods of the 1st and 2nd spectral peaks and also the half period of the 1st peak (see legend). Arrows indicate the direction (relative to N) of coherent microseismic waves. c) Weather map representative of this storm. d) Comparison of data from weather ship and power variations of the 1st and 2nd microseismic peak (see legend).

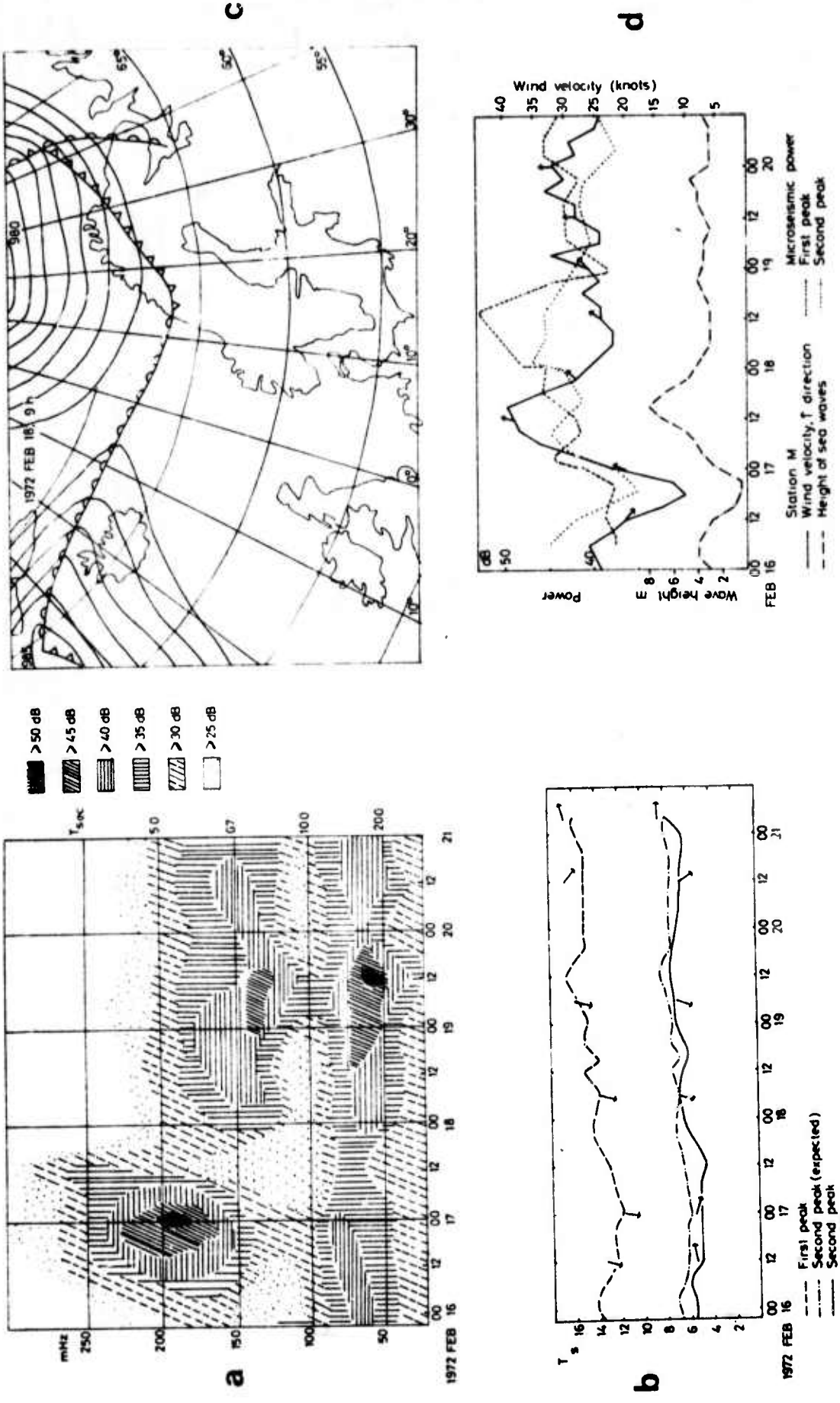

Fig. 6 Pictorial synopsis of Storm 2. See caption for Fig. 5.

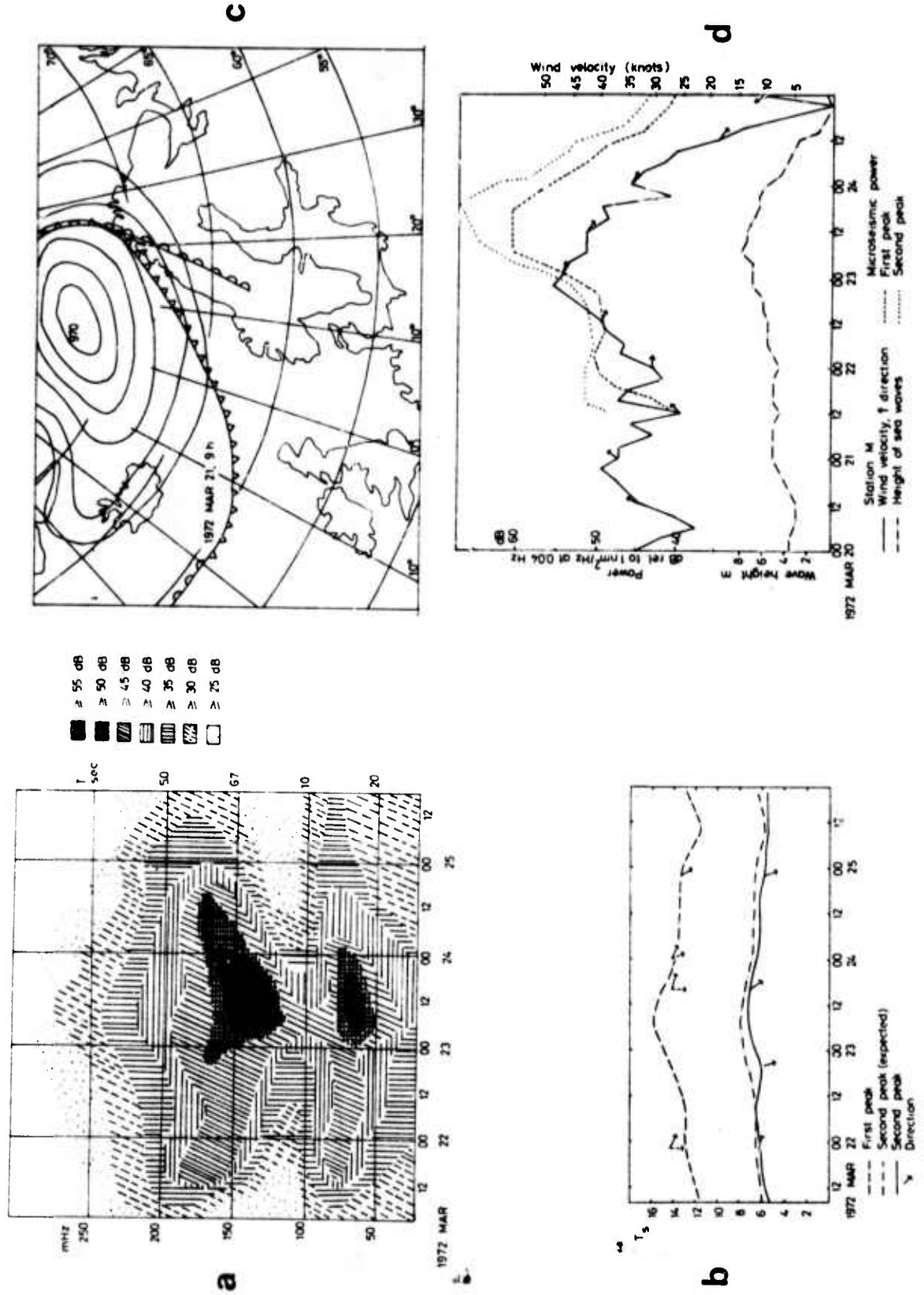

Fig. 7 Pictorial synopsis of Storm 3. See caption for Fig. 5.

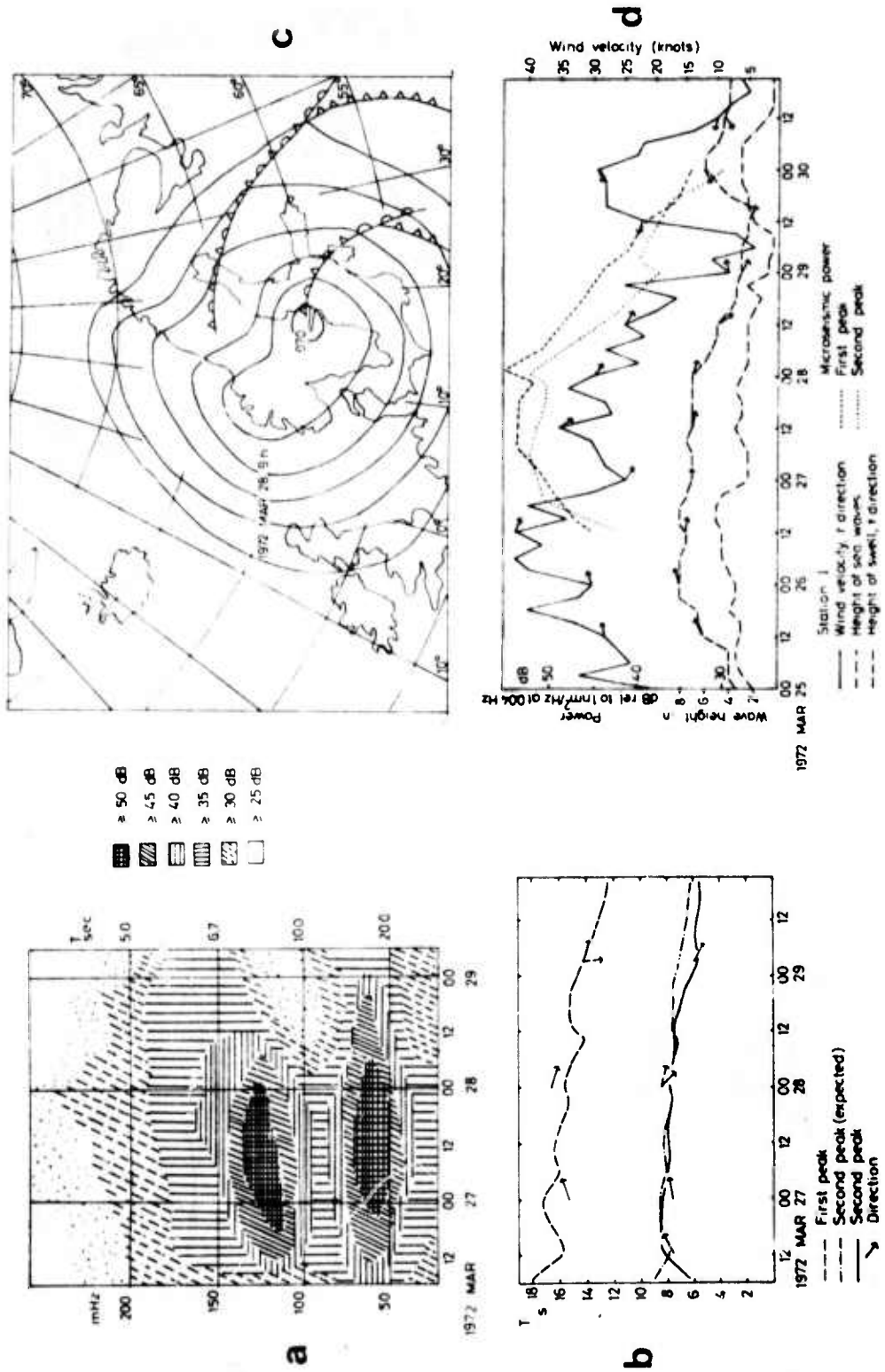

Fig. 8 Pictorial synopsis of Storm 4. See caption for Fig. 5.

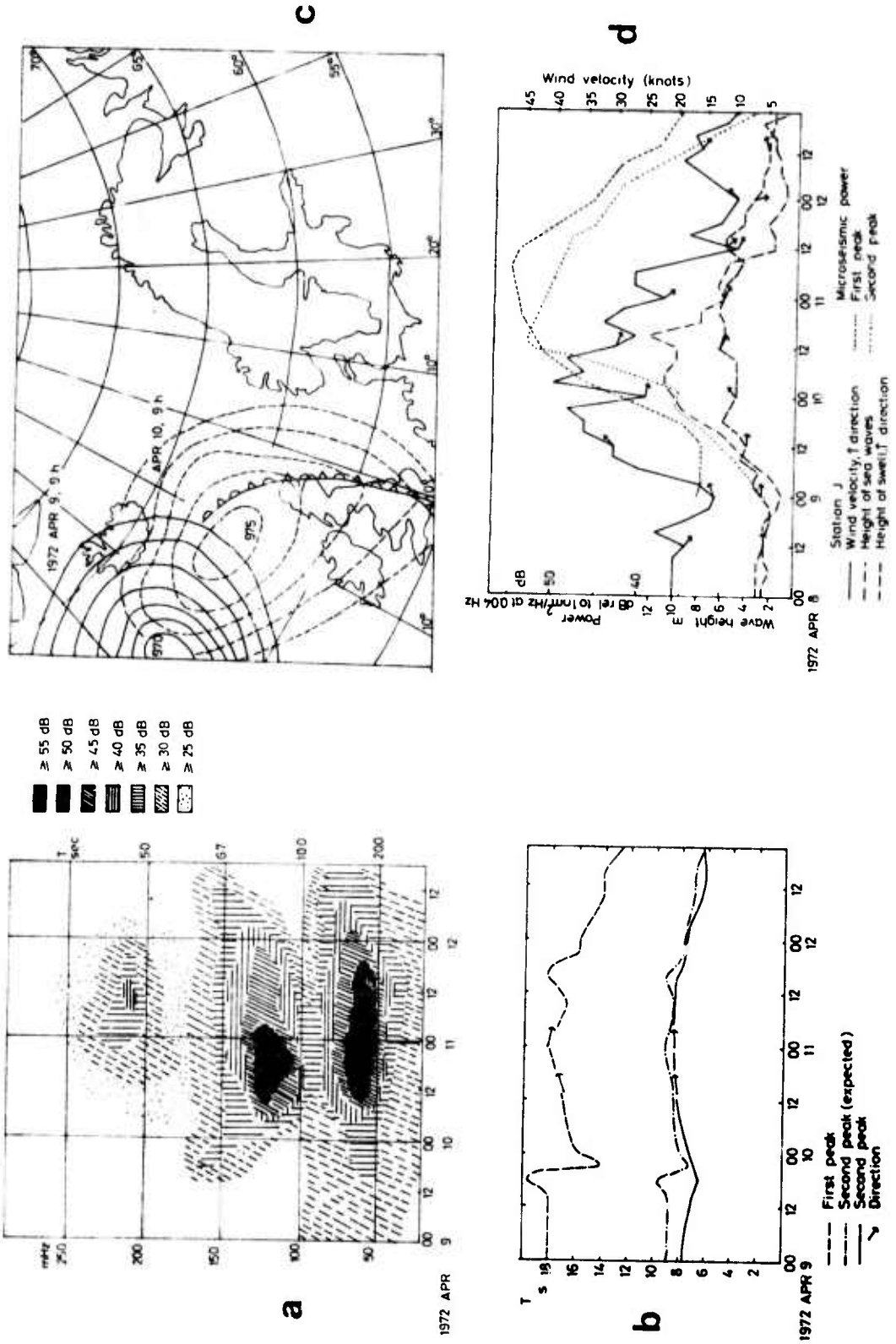

Fig. 9 Pictorial synopsis of Storm 5. See caption for Fig. 5.

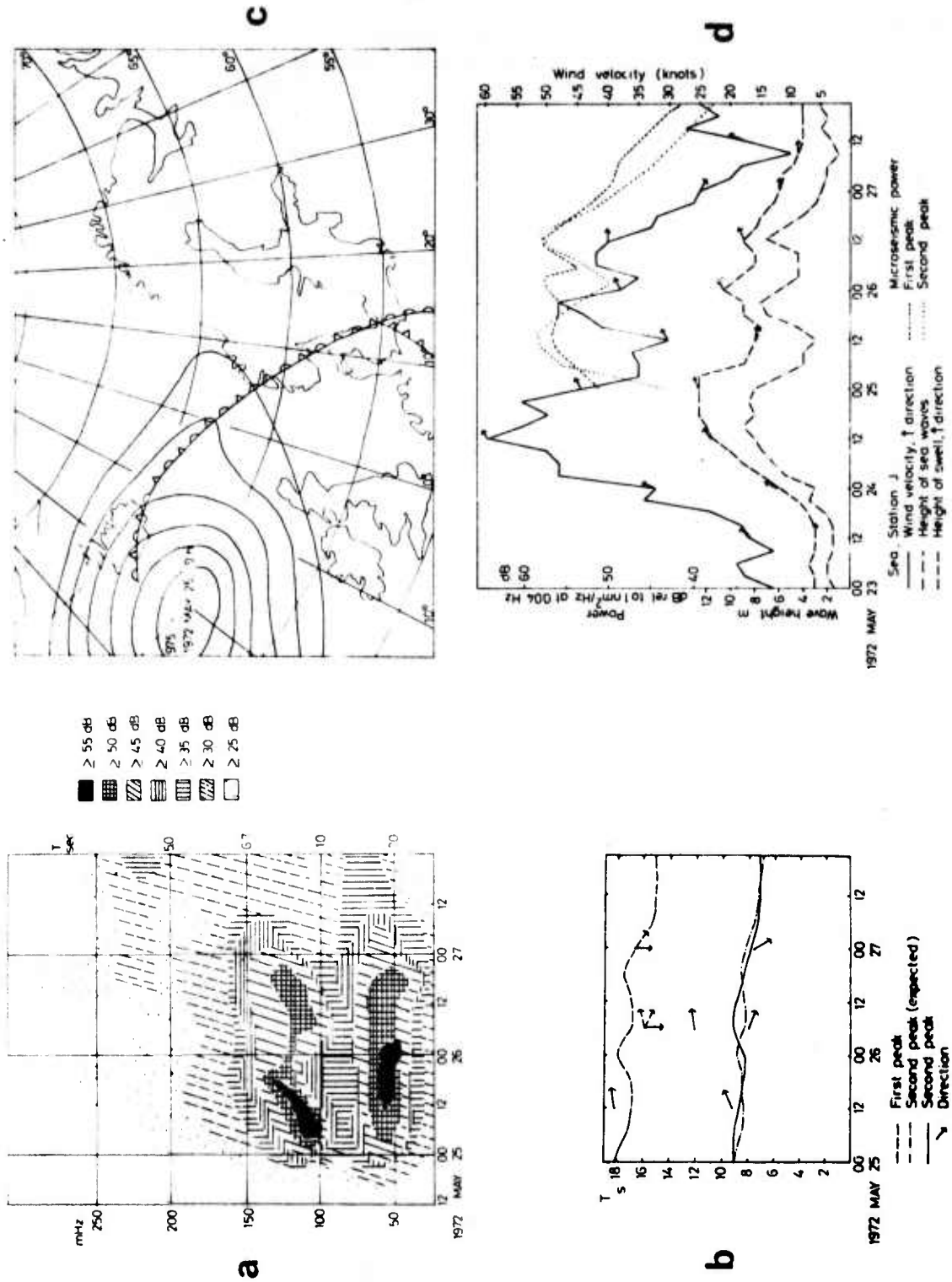

Fig. 10 Pictorial synopsis of Storm 6. See caption for Fig. 5.

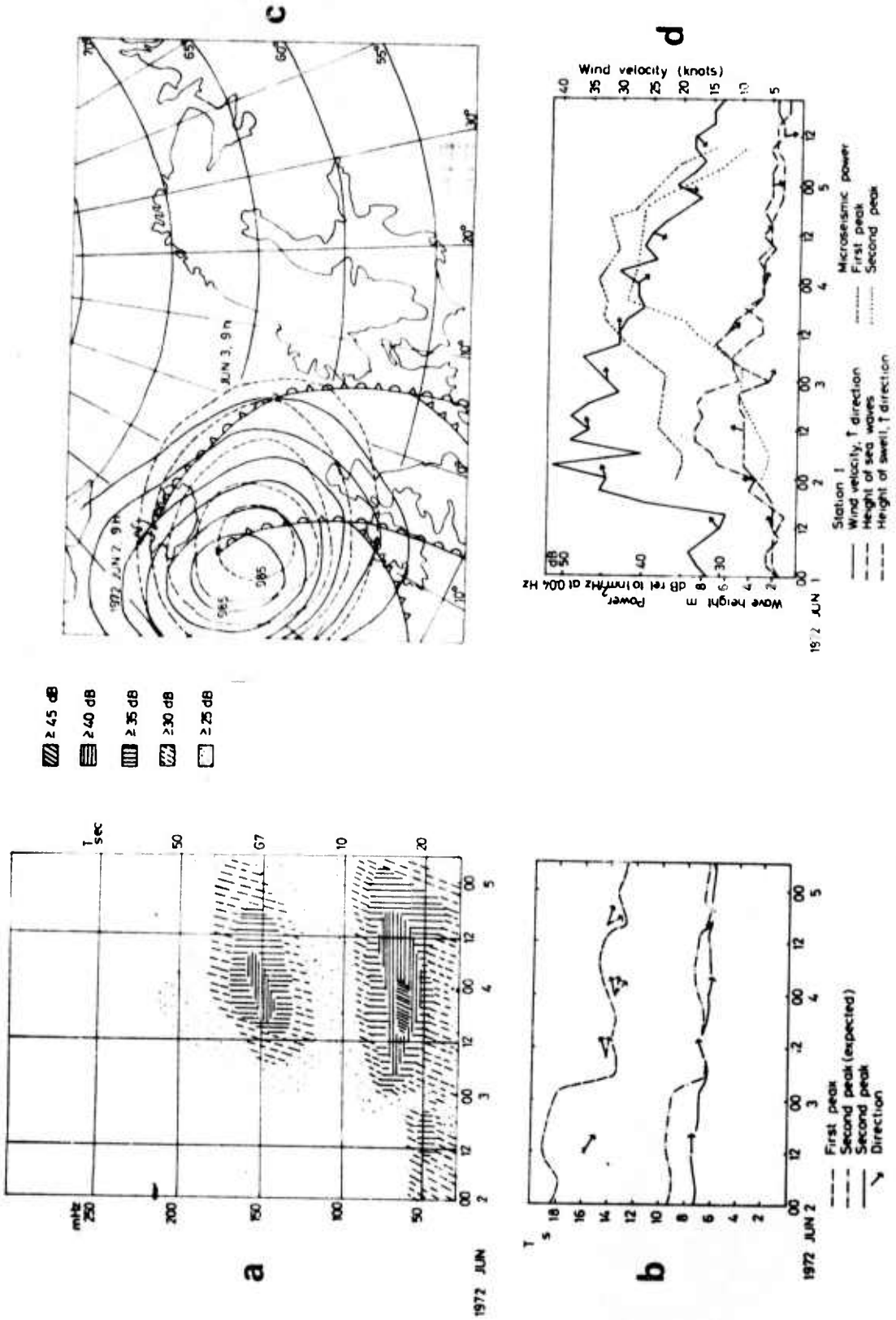

Fig. 11 Pictorial synopsis of Storm 7. See caption for Fig. 5.

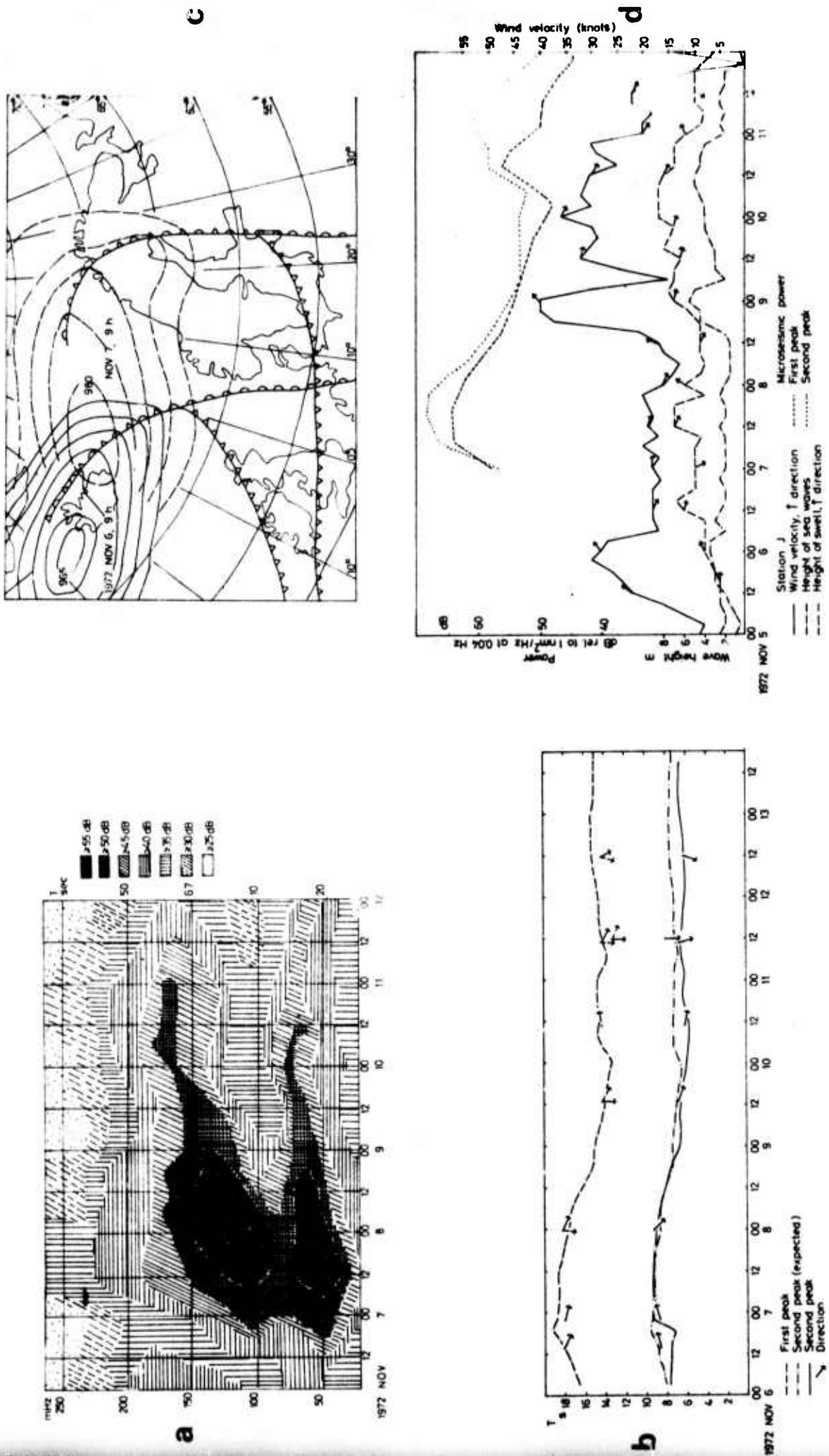

Fig. 12 Pictorial synopsis of storm 8. See caption for Fig. 5.

3.3 Primary frequency peak (1st peak)

The origin of this low frequency peak is generally attributed to the approaching of ocean waves into shallow water areas. Thus these primary frequency microseisms should occur at the same periods as the corresponding ocean waves (Haubrich et al, 1963; Hasselmann, 1963; Båth, 1974). As mentioned above, however, the ocean wave data available to us are insufficient for detailed examination of this hypothesis. The low frequency microseisms could also be generated by cold fronts passing the NORSAR array (Bungum, 1974) or the Norwegian coast.

One of the most important features in the NORSAR long period microseismic spectra, especially from the point of view of detection seismology, is the existence of strong first peak in the low frequency part of the spectrum, with peak frequencies in the band 50-85 mHz and power levels between 35-65 dB. Especially in the beginning of storm developments from the North Atlantic Ocean, this peak dominates the spectrum. The wave-number spectra in these cases show well-concentrated source areas with azimuthal angles 230^{o}-270^{o} and with peak frequencies at 50-65 mHz (storms 4, 5, 6 and 7). Thus these microseisms are probably generated at the coastal waters to the west and north of the British Isles. In the later development of the storms, this peak shifts towards higher frequencies, within the band 60-85 mHz. Simultaneously the wave-number spectra show broadened source areas from W to N of NORSAR. This seems to indicate that the sources have moved from the North Atlantic Ocean and into the Norwegian Sea, approaching the coastal areas of Norway. In some cases this is surprising because no large swell and surf are observed at the Norwegian Sea.

When a meteorological storm is confined to the Norwegian Sea and nearby coastal areas (storms 2,3), the 1st peak appears at frequencies around 60-85 mHz and there is a clear shift

of peak frequencies towards lower values with subsequent increase in power. Wave-number analyses show broad source areas for these microseisms in the direction 0-20° for storm 2 and 300-360° for storm 3. Thus these microseisms are probably generated mainly at or close to the shallow water areas between northern Norway and Svalbard.

3.4 Double frequency peak (2nd peak)

In all the microseismic storm spectra obtained in this study, there occurs a clear maximum at frequencies around 110-195 mHz, with power ranging from 25 dB to 65 dB. This peak represents the "ordinary" microseisms investigated in Europe by many authors (see, for example, Båth, 1952, 1962; Zátopek, 1964; Kulhánek and Båth, 1972).

In the development of storms originating in the North Atlantic Ocean (storms 1, 4, 5, 6 and 7) the power of the 2nd peak, as observed at NORSAR, is generally 5-10 dB below that of the 1st peak. Wave-number analyses in these cases show well-concentrated sources, and in the same general directions as those of lower frequency peaks. During the later development of the storms, more diffuse sources appear to the west and north suggesting that the source area(s) has migrated into the Norwegian Sea. Simultaneously the peak frequencies migrate towards the frequency band 140-195 mHz.

During the Norwegian Sea storms (storm 2, 3 and 8), the frequencies of the 2nd peak all occur in the band 130-195 mHz. The power level is generally equal to or higher than that of the low frequency peak. The majority of the peak frequencies of the first and second peak are reasonably consistent with the ratio 1:2 (see Tables 1 and 2), and in the few cases where the ratio is significantly different from 2, it is always greater, i.e., the observed periods of the 2nd peak are somewhat smaller than expected (see Figs. 5b-12b).

That effect will not be compensated for, but rather enhanced by, introducing corrections for instrumental response since these will decrease the period of the 2nd peak more than that of the 1st peak.

In most cases the wave-number analysis points towards the same source areas for 1st and 2nd peak microseisms. The problem of whether or not their generation mechanism is the same remains open. The second peak could be due to standing wave oscillations according to Longuet-Higgins theory or the first and second peak could be fundamental and second harmonics both due to coast effects (Båth, 1974).

3.5 Storm development

Two different storm development models can be derived from the present spectral analysis of NORSAR microseisms. The first of them shows a U-shaped character in the sonograms (storms 2, 3 and 8) and are associated mainly with the Norwegian Sea storms. They usually begin with a shift of peak frequencies towards lower values, when the power of the storm increases. This shift is clearest at the 2nd peak but also present on the 1st.

In the other development model the peak power which at first occurs at lower frequencies shifts continuously towards higher frequencies as the storm develops (storms 1, 4, 5, 6 and 7). These storms are characterized with a source approaching from the North Atlantic Ocean towards the Norwegian Sea and coast. In all these cases the wind velocities over the North Atlantic Ocean are up to 40-60 knots, the direction of the wind being most often from W-SW towards the coast of the British Isles and later on Norway. This shift of peak frequencies could be partly due to swell dispersion (Haubrich et al, 1963).

For some of the storms investigated in this paper there also occurs a 3rd peak in the high frequency part of the spectrum

(storms 5 and 6). This peak is found also in studies of Oulu microseisms (Korhonen, 1971), where all the three peaks are sometimes found to shift simultaneously during the storm development. At NORSAR the wave-number analysis shows for the 3rd peak microseisms approximately the same direction of approach as for the 1st and 2nd peaks. These observations support the idea that all the three peaks could be generated in the same source area. In some cases, however, the overlapping of different sources seems to be more probable.

Generally there is a time lag of up to 48 hours between the maxima of the wind and the microseisms and up to 24 hours between the maxima of the ocean waves and the microseisms. In addition there is a tendency for the first microseismic maximum to precede the second and third maxima in time.

4. CONCLUSIONS

The following is a summary of observations and interpretations which can be made from the results presented in this report:

1. Spectra of storm microseisms at NORSAR show a clearly peaked character. Most of the spectra are double-peaked but sometimes three peaks are evident. The same spectral character has also been found at Fennoscandian single stations. In the NORSAR spectra, however, the low frequency peak often yields higher power levels than other peaks on account of instrumental response.

2. Stronger storms, as investigated by frequency wave-number analysis, usually provide concentrated peaks with narrower peak widths than weaker storms, which is to be expected as an effect of the higher coherency of the waves in the former case.

3. The microseismic storms can be divided into two development models. U-shaped sonograms seem to be associated with the Norwegian Sea storms whereas for the North Atlantic Ocean storms a continuous shift of peak frequencies towards higher values is found.

4. In the first phase of the North Atlantic Ocean storms the peak frequencies are found in the band 50-65 mHz for the 1st peak and at 110-140 mHz for the 2nd peak. In these spectra there sometimes also occurs a 3rd peak at even higher frequencies around 180-250 mHz.

5. During the Norwegian Sea storms the 1st peak occurs in the band 65-85 mHz, and the second peak in the band 130-195 mHz.

6. The ratio of the peak frequencies of the 1st and 2nd peak is usually not significantly different from 1:2, which is in accordance with theories for generation mechanisms.

7. During the North Atlantic Ocean storms the 1st peak occurs at a higher power level than the 2nd peak, whereas the opposite usually holds for the Norwegian storms.

8. In the beginning of the North Atlantic Ocean storms, frequency wave-number analyses indicate well-concentrated source areas with azimuthal angle 230°-270° for both the 1st and the 2nd microseismic peaks. We suggest that these microseisms are generated at the deep water boundary to the west and north of the British Isles. In the later development of the storms the wave-number spectra indicate an effective broadening of the source area, which is in accordance with the increasing proximity of the storm to the NORSAR array. In addition, a new source appears to the north of NORSAR, which may be due to swells in the corresponding coastal areas.

9. During the storms of the Norwegian Sea the wave-number analyses indicate diffuse sources within the wide azimuthal range 270°-20°, pointing towards the coastal area of Norway and the deep water boundaries between northern Norway and Svalbard as the most probable areas for the generation of these waves.

ACKNOWLEDGEMENTS

This research is part of a program of cooperation in detection seismology among Nordic countries. The authors wish to express their gratitude to NTNF/NORSAR for use of the NORSAR data processing facilities. This work has been supported financially by the Ministry of Education of Finland and by the Finnish Academy, State Committee of Natural Sciences.

The authors are also grateful to the NORSAR scientists for much valuable advice and many discussions. The assistance of Dr. Hilmar Bungum during the various phases of this work, especially his comments to and critical reading of the manuscript are appreciated. Annukka Karinen drew the figures.

REFERENCES

Bernard, P. (1941): Sur certaines propriétés de la houle étudices à l'aide des enregistrements seismographiques, Bull. Inst. Océanographique Monaco, No. 800, 1-19.

Bungum, H., L. Bruland and E. Rygg (1971): Short-period seismic noise structure at Norwegian Seismic Array, Bull. Seism. Soc. Am., 61, 357-373.

Bungum, H., E.S. Husebye and F. Ringdal (1971): The NORSAR array and preliminary results of data analysis, Geophys. J.R. Astr. Soc., 25, 115-126.

Bungum, H., and J. Capon (1974): Coda pattern and multipath propagation of waves at NORSAR, Phys. Earth Planet. Int., 9, 111-127.

Bungum, H. (1974): Array station as a tool for microseismic research. The XIII General Assembly of the European Seismological Commission, Part I, 231-241, Geological Institute, Technical and Economical Studies D series, No. 10.

Båth, M. (1952): Review over investigations of microseisms in Scandinavia, Pont. Acad. Sci., Scripta Varia 12, 239-276.

Båth, M. (1962): Direction of approach of microseisms. Geophys. J.R.Astr. Soc., 6,

Båth, M. (1974): Spectral analysis in geophysics, Developments in solid earth geophysics, 7, Elsevier, 1156.

Capon, J. (1969): High-resolution frequency-wavenumber spectrum analysis, Proceedings of the IEEE, 57, 1408-1418.

Capon, J. (1972): Long-period signal processing results for LASA, NORSAR and ALPA, Geophys. J.R. Astr. Soc., 31, 279-296.

Darbyshire, J., and E.O. Okeke (1969): A study of primary and secondary microseisms recorded in Anglesey, Geophys. J.R. Astr. Soc., 17, 63-92.

Hasselmann, K. (1963): Statistical analysis of the generation of microseisms, Rev. of Geophys., 1, 177-210.

Haubrich, R.A., W.H. Munk and F.E. Snodgrass (1963): Comparative spectra of microseisms and swell, Bull. Seism. Soc. Am., 53, 27-37.

Hinde, B.J., and D.I. Gaunt (1966): Some new techniques for recording and analysing microseisms, Proc. R.Soc. London A 290.

Korhonen, H. (1971): Types of storm microseism spectra at Oulu, Contrib. no. 15, Dept. of Geophys., University of Oulu, Finland.

Korhonen, H., and S.E. Pirhonen (1974): Three peaked storm microseism spectra. IASPEI, Commission des Microseismes, Premier Rapport, edited by P. Bernard, Paris.

Kulhánek, O., and M. Båth (1972): Power spectra and geographical distribution of short-period microseisms in Sweden, PAGEOPH, 94, 148-171.

Longuet-Higgins, M.S. (1950): A theory on the origin of microseisms, Phil. Trans. Roy. Soc. London, A. 243, 1-35.

Rygg, E., and L. Bruland (1974): Long period microseisms in southern Norway, Scientific Report No. 10, ARPA Order No. 1827-10, Seismological Observatory, University of Bergen, 1-41.

Wiechert, E. (1904): Verhandlungen der zweiten internationalen Seismologischen Konferenz, Gerlands Beitr. Geophy., Erg.-Bd. II, 1904, 41-43.

Zátopek, A. (1964): Long-period microseisms generated in the eastern part of the Atlantic frontal zone. Studia geoph. et Geod., 8, 127-139.